AD-A121 672 ELASTIC CONSTANTS OF QUARTZ(U) ROME AIR DEVELOPMENT 1/1
CENTER GRIFFISS AFB NY A KAHAN MAY 82 RADC-TR-82-117

UNCLASSIFIED F/G 20/11 NL

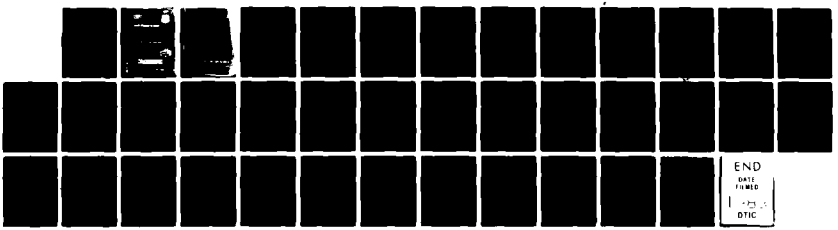

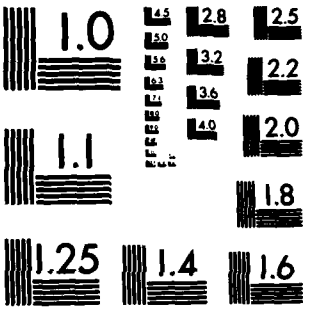

[illegible]

RADC-TR-[illegible]

APPROVED:

[illegible] D. [illegible], Jr.
Chief, Elect [illegible] Branch
Solid State Sciences Division

APPROVED:

HAROLD ROTH
Director, Solid State Sciences Division

FOR THE COMMANDER:

[illegible]

Unclassified

SECURITY CLASSIFICATION OF THIS PAGE (When Data Entered)

REPORT DOCUMENTATION PAGE	READ INSTRUCTIONS BEFORE COMPLETING FORM
1 REPORT NUMBER: RADC-TR-82-117	2. GOVT ACCESSION NO.: AD-A121672
	3 RECIPIENT'S CATALOG NUMBER:
4 TITLE (and Subtitle): ELASTIC CONSTANTS OF QUARTZ	5. TYPE OF REPORT & PERIOD COVERED: In-House
	6 PERFORMING ORG. REPORT NUMBER:
7 AUTHOR(s): Alfred Kahan	8. CONTRACT OR GRANT NUMBER(s):
9. PERFORMING ORGANIZATION NAME AND ADDRESS: Deputy for Electronic Technology (RADC/ESE) Hanscom AFB Massachusetts 01731	10. PROGRAM ELEMENT, PROJECT, TASK AREA & WORK UNIT NUMBERS: 61102F 2305J104
11. CONTROLLING OFFICE NAME AND ADDRESS: Deputy for Electronic Technology (RADC/ESE) Hanscom AFB Massachusetts 01731	12. REPORT DATE: May 1982 13. NUMBER OF PAGES: 38
14. MONITORING AGENCY NAME & ADDRESS(if different from Controlling Office):	15. SECURITY CLASS. (of this report): Unclassified 15a. DECLASSIFICATION DOWNGRADING SCHEDULE:

16. DISTRIBUTION STATEMENT (of this Report)

Approved for public release, distribution unlimited

17. DISTRIBUTION STATEMENT (of the abstract entered in Block 20, if different from Report)

18 SUPPLEMENTARY NOTES

19 KEY WORDS (Continue on reverse side if necessary and identify by block number)

Quartz
Material properties
Crystal resonators
Wave propagation
Frequency standard

20 ABSTRACT (Continue on reverse side if necessary and identify by block number)

The formalism describing the thickness vibrations of anisotropic piezoelectric infinite plates is reviewed. The mathematical treatment is specialized to crystallographically doubly-rotated quartz. Explicit expressions for the piezoelectrically "stiffened" elastic constants are derived. The validity of currently accepted elastic constant values is discussed. It is concluded that there is a need to redetermine the constants and their temperature coefficients on a geometrically consistent sample set using piezoelectric excitation.

DD FORM 1 JAN 73 1473 EDITION OF 1 NOV 65 IS OBSOLETE

Unclassified

SECURITY CLASSIFICATION OF THIS PAGE (When Data Entered)

Preface

The author is indebted to Dr. A. Ballato for invaluable discussions. Needless to say, the opinions expressed in this report regarding the Bechmann, Ballato, and Lukaszek publications reflect the author's views and not necessarily those of Dr. Ballato. Thanks are also due to Dr. A. Slobodnik for discussions and for performing comparative numerical analysis, using his bulk wave propagation computer program. Appreciation is expressed to Dr. G. Schmidt of Lowell Institute for checking the extensive algebra involved in deriving the explicit expressions for the "stiffened" elastic constants.

Contents

Illustrations

Tables

Elastic Constants of Quartz

1. INTRODUCTION

The critical performance characteristics of a crystal resonator device, frequency, electromechanical coupling, and temperature sensitivity, are determined by the elastic, piezoelectric, and dielectric constants of the material and their temperature coefficients. In this investigation we consider the influence of the material coefficients on the thickness vibrations of crystallographically doubly rotated quartz. The simplest mathematical formalism that describes a vibrating infinite plate with appropriate boundary conditions relates the measured frequencies to the material constants. The set of four coupled differential equations yields a set of linear equations for the displacement and results in three eigenvalues for the phase velocities. The general formulation of this approach is outlined, for example, in Tiersten.[1]

For an arbitrary doubly rotated quartz cut, the vibration frequencies are determined by ten independent fundamental material constants: six elastic, two piezoelectric, and two dielectric. In turn, the vibration frequencies can be used in conjunction with the mathematical formalism to derive numerical values for the

(Received for publication 13 May 1982)

1. Tiersten, H. F. (1969) Linear Piezoelectric Plate Vibrations, Plenum Press, pp. 88-93.

material properties. The derived material values are mathematical-formalism dependent, and they may differ from the intrinsic constants.

For highly symmetric crystal orientations, the cubic equation for the frequency eigenvalues can be factored, and the number of material constants involved in determining the vibration frequencies is drastically reduced. In some cases the resulting frequency depends on a single elastic constant. These directions, designated as the uncoupled mode orientations, are the ones most often utilized for the experimental determination of the elastic constants.

The experimental determination of the elastic constants of quartz has occupied many investigators over long periods of time. Cady[2] reviews several approaches and lists corresponding numerical values. Reference 2 is a corrected reprint of the original treatise published on the subject of piezoelectricity in 1946, and the listed values are the ones accepted in 1946. Currently, the most widely accepted elastic constant values are the ones determined by McSkimin,[3] and independently by Bechmann, Ballato, and Lukaszek.[4] [This reference is hereafter abbreviated as BBL (1962)]. McSkimin has applied ultrasonic excitation to bulk crystals along the uncoupled directions, whereas BBL utilized piezoelectric excitation and doubly rotated crystal disks in a resonator configuration. Both investigators used the same mathematical description to relate experimental wave velocities to the elastic constants. The elastic constants determined by these investigators agree with each other, and also generally agree with previous results.

We have applied a least squares analysis to the BBL (1962) data set and we find major discrepancies between the listed values and the least squares fit derived constants. This raises serious questions with respect to the validity of the material values and their applicability to crystallographically doubly rotated, piezoelectrically excited resonators.

2. THICKNESS VIBRATIONS OF PIEZOELECTRIC PLATES

Tiersten[1] has derived the differential equations for the thickness vibrations of an arbitrarily anisotropic, piezoelectric, infinite plate. The wave propagation is described by a set of four coupled linear equations in four variables u_j and Φ

2. Cady, W.G. (1964) Piezoelectricity, Dover Publications, Vol. I, pp. 134-157.
3. McSkimin, H.J. (1962) Measurement of the 25°C zero-field electric moduli of quartz by high frequency plane-wave propagation, J. Acoust. Soc. Am. 34:1271-1274.
4. Bechmann, R., Ballato, A.D., and Lukaszek, T.J. (1962) Higher-order temperature coefficients of the elastic stiffnesses and compliances of alpha-quartz, Proc. of the IRE 50:1812-1822.

$$c'_{\nu jk\nu}\frac{\partial^2 u_k}{\partial x_\nu^2} + e'_{\nu\nu j}\frac{\partial^2 \Phi}{\partial x_\nu^2} = \rho\frac{\partial^2 u_j}{\partial t^2} \tag{1}$$

$$e'_{\nu\nu k}\frac{\partial^2 u_k}{\partial x_\nu^2} - \varepsilon'_{\nu\nu}\frac{\partial^2 \Phi}{\partial x_\nu^2} = 0 \tag{2}$$

where $c'_{\nu jk\nu}$, $e'_{\nu\nu j}$, and $\varepsilon'_{\nu\nu}$ are the elastic, piezoelectric, and dielectric constants, ρ denotes the density, u_j the components of the displacement vector, Φ the electromagnetic scalar potential, x_ν the spatial coordinates, and t the time. The primed notation on the material constants indicate that these quantities are referred to the rotated wave propagation coordinate system. A standard tensor convention is used in subscripts, namely, repeated Latin indices imply summation over 1, 2, and 3, but no summation is implied over repeated Greek indices. In succeeding equations we also adopt the notations of indicating differentiation with respect to space coordinates by commas followed by an index and time derivatives by dots over the variables.

The boundary conditions applicable to this problem, a forcing alternating voltage and vanishing mechanical stresses at the plate surfaces, $x_\nu = \pm h$, are

$$\Phi = \pm\Phi_o \cos\omega t \tag{3}$$

$$T_{\nu j} = c'_{\nu jk\nu}\frac{\partial u_k}{\partial x_\nu} + e'_{\nu\nu j}\frac{\partial \Phi}{\partial x_\nu} = 0 \tag{4}$$

where $T_{j\nu}$ is the stress tensor, and 2h, the plate thickness.

The piezoelectrically "stiffened" elastic constant is defined

$$\Gamma_{\nu jk\nu} = c'_{\nu jk\nu} + e'_{\nu\nu j}\, e'_{\nu\nu k}/\varepsilon'_{\nu\nu} \tag{5}$$

In terms of $\Gamma_{\nu jk\nu}$, Eqs. (1) and (2) combine to form a set of three linear coupled equations

$$\Gamma_{\nu jk\nu}\frac{\partial^2 u_k}{\partial x_\nu^2} = \rho\ddot{u}_j \tag{6}$$

Tiersten shows that a solution to the differential equations based on a linear combination of symmetric and antisymmetric plain waves remains uncoupled, and, moreover, that the symmetric waves cannot be excited by the application of an alternating voltage to the surface electrodes. Consequently, it is mathematically

rigorous to assume that the solution is a set of antisymmetric plain waves in the form

$$u_j(x_\nu, t) = u_j(x_\nu) \cos \omega t = \beta_j \sin (\omega/v)\, x_\nu \cos \omega t \tag{7}$$

$$\Phi(x_\nu, t) = \Phi(x_\nu) \cos \omega t \tag{8}$$

Substituting these expressions into Eq. (6), yields the set of three equations

$$(\Gamma_{\nu jk\nu} - \delta_{jk}\Gamma)\beta_k = 0 \qquad j, k = 1, 2, 3 \tag{9}$$

where the eigenvalue Γ is related to the phase velocity v by

$$\Gamma = \rho v^2 \tag{10}$$

The three eigenvalues Γ are obtained by expanding the 3 × 3 determinant

$$\left|\Gamma_{\nu jk\nu} - \delta_{jk}\Gamma\right| = 0 \tag{11}$$

and solving the resulting cubic equation for Γ^m, m = 1, 2, and 3. For a given frequency ω there are three independent transverse velocities.

For a given eigenvalue Γ^m and eigenvector β_j^m, the electromagnetic potential is determined from the boundary conditions of Eq. (3). This results in

$$\Phi^m(x_\nu) = (e'_{\nu\nu j}/\varepsilon'_{\nu\nu})\, u_j^m(x_\nu) + L_1 x_\nu/h \tag{12}$$

where the integration constant L_1 is

$$L_1 = \Phi_o - (e'_{\nu\nu j}/\varepsilon'_{\nu\nu})\, \beta_j^m \sin (\omega h/v^m) \tag{13}$$

The short-circuit resonance frequencies are found from the six stress boundary conditions implied in Eq. (4). They are the solutions of the transcendental equation

$$\sum_{m=1}^{3} (k^m)^2 \frac{\tan (\omega h/v^m)}{(\omega h/v^m)} = 1 \tag{14}$$

where for a given mode m the electromechanical coupling factor k^m is defined as

$$(k^m)^2 = (e'_{\nu\nu j}\, \beta_j^m)^2/(\varepsilon'_{\nu\nu}\, \Gamma^m) \qquad m = 1, 2, 3 \tag{15}$$

The sum $e'_{\nu n_j} \beta_j^m$ is the effective piezoelectric constant, and it determines the excitation magnitude of the mode. In general, the resonance frequencies cannot be attributed to a particular mode, but are coupled functions of all three modes. Ballato[5] reviewed the regions in which different approximations applicable to the resonance equation are valid.

3. COORDINATE SYSTEMS AND TRANSFORMATION MATRICES

Figure 1 depicts the plate geometry and crystallographic coordinate system used in this investigation. We assume $x_1 = x$, $x_2 = y$, and $x_3 = z$, with x_1 and x_3 in the plane of the plate. The phase velocity propagates along x_2, normal to the plate. The initial position of the plate is a Y-cut, with its thickness direction normal to the y-axis. The position of the rotated plate is described by angles (ϕ, θ), where ϕ and θ are rotations around the z- and x-axis, respectively.

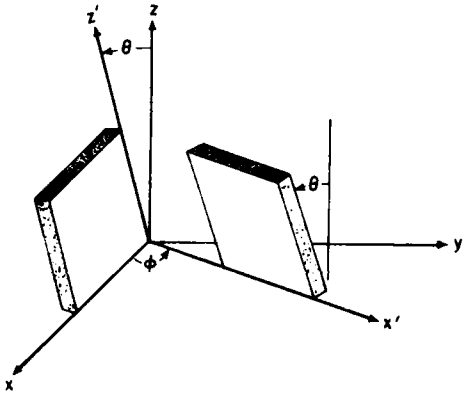

Figure 1. Coordinate System for a Doubly Rotated Plate

The wave propagation and crystallographic coordinate systems are related by a transformation matrix V_{ij}. The V_{ij} matrix elements are defined by the dot products of the orthogonal unit vectors of the two systems. The direction cosines for a ϕ-rotation around the z-axis are given by

$$a_{ij} = \begin{bmatrix} \cos\phi & \sin\phi & 0 \\ -\sin\phi & \cos\phi & 0 \\ 0 & 0 & 1 \end{bmatrix} \tag{16}$$

5. Ballato, A. (1977) Doubly rotated thickness mode plate vibrators, Physical Acoustics, XIII, W. P. Mason and R. N. Thurston, Eds., Academic Press, New York, pp. 115-181.

and for a θ-rotation around the x-axis by

$$b_{ij} = \begin{bmatrix} 1 & 0 & 0 \\ 0 & \cos\theta & \sin\theta \\ 0 & -\sin\theta & \cos\theta \end{bmatrix} \tag{17}$$

For a doubly rotated crystal plate, a ϕ-rotation followed by a θ-rotation, the transformation matrix $V_{ij} = b_{ik}a_{kj}$ connecting the wave propagation and crystallographic coordinate systems becomes

$$V_{ij} = \begin{bmatrix} \cos\phi & \sin\phi & 0 \\ -\sin\phi\cos\theta & \cos\phi\cos\theta & \sin\theta \\ \sin\phi\sin\theta & -\cos\phi\sin\theta & \cos\theta \end{bmatrix} \tag{18}$$

The material properties appearing in the differential equations are described by 2, 3, or 4 subscripts. We introduce the compressed subscript notation, replacing ij or kl by p or q, according to the prescription given in Table 1. This allows the material constants to be described by two subscripts and expressed as matrices.

Table 1. Relationship Between Subscripts i, j, k, l, and p, q

ij or kl	p or q
11	1
22	2
33	3
23 or 32	4
13 or 31	5
12 or 21	6

The primed material constants referred to in the wave propagation system are related to quantities in the crystallographic reference system by second, third, or fourth rank tensor transformations. More specifically,

$$\epsilon'_{ij} = V_{im} V_{jn} \epsilon_{mn} \tag{19}$$

$$e'_{ip} = e'_{ijk} = V_{im} V_{jn} V_{ko} e_{mno} \tag{20}$$

$$c'_{pq} = c'_{ijkl} = V_{im} V_{jn} V_{ko} V_{lp} c_{mnop} \tag{21}$$

where V_{ij} are the rotation matrix elements of Eq. (18), and the repeated subscript indices imply summations over 1, 2, and 3. Thus each ε'_{ij}, e'_{ip}, and c'_{pq} element is the sum of 9, 27, and 81 terms, respectively.

In the pq notation, ε is described by a 3×3 matrix with 9 elements, e by a 3×6 matrix with 18 elements, and c by a 6×6 matrix with 36 elements. However, for any crystal system the number of independent matrix elements is reduced by symmetry. For example, for the most general crystal system, a triclinic system without a center of symmetry, the applicable symmetries are:

$$\varepsilon_{ij} = \varepsilon_{ji} \tag{22}$$

$$e_{ijk} = e_{ikj} \tag{23}$$

$$c_{ijkl} = c_{ijlk} = c_{jikl} = c_{klij} \text{ or } c_{pq} = c_{qp} \tag{24}$$

The number of independent constants are thus reduced to 45 (6 dielectric, 18 piezoelectric, and 21 elastic). The number of independent material constants are further reduced with increasing crystal symmetry.

The material of primary interest to this investigation is α-quartz. This trigonal crystal system, (32, class D_3), has a three-fold symmetry with respect to the z-axis and a two-fold symmetry with respect to the x-axis. The material properties are invariant under a 120° rotation around the z-axis or a 180° rotation around the x-axis. Using these transformation properties, it can be shown that the number of independent material constants reduce to 10, 2 dielectric, 2 piezoelectric, and 6 elastic. The material matrix arrays applicable to α-quartz are listed in Table 2. The structure of these arrays also holds true for other material properties transforming as second, third, or fourth order tensors. For example, the array for the linear expansion coefficient α_{ij} has the same matrix structure as ε_{ij}.

Table 2. Material Arrays for α-Quartz

Dielectric Constants

$$\varepsilon_{ij} = \begin{bmatrix} \varepsilon_{11} & 0 & 0 \\ 0 & \varepsilon_{11} & 0 \\ 0 & 0 & \varepsilon_{33} \end{bmatrix}$$

Piezoelectric Constants

$$e_{ip} = \begin{bmatrix} e_{11} & -e_{11} & 0 & e_{14} & 0 & 0 \\ 0 & 0 & 0 & 0 & -e_{14} & -e_{11} \\ 0 & 0 & 0 & 0 & 0 & 0 \end{bmatrix}$$

Elastic Constants

$$c_{pq} = \begin{bmatrix} c_{11} & c_{12} & c_{13} & c_{14} & 0 & 0 \\ c_{12} & c_{11} & c_{13} & -c_{14} & 0 & 0 \\ c_{13} & c_{13} & c_{33} & 0 & 0 & 0 \\ c_{14} & -c_{14} & 0 & c_{44} & 0 & 0 \\ 0 & 0 & 0 & 0 & c_{44} & c_{14} \\ 0 & 0 & 0 & 0 & c_{14} & c_{66} \end{bmatrix}$$

where $c_{66} = (c_{11} - c_{12})/2$

One can derive explicit algebraic expressions for the "rotated" material constants of Eqs. (19), (20), and (21), by applying the rotation matrix V_{ij} to the arrays listed in Table 2. The results, for the material components of interest to this investigation, are listed in Table 3. For quartz, owing to crystal symmetry, all rotations can be mapped into

$$0 \leq \phi \leq 60^{\circ} \quad \text{and} \quad 0 \leq \theta \leq 90^{\circ}$$

In this nomenclature, the standard AT-cut crystal is designated as $(0, \sim 35)^{\circ}$ and the BT-cut as $(60, \sim 49)^{\circ}$. Another commonly used mapping region is

$$0 \leq \phi \leq 30^{\circ} \qquad \text{and} \qquad -90 \leq \theta \leq 90^{\circ}$$

The two descriptions are related by the transformations

$$\phi \rightarrow 60^{\circ} - \phi \qquad \text{and} \qquad \theta \rightarrow -\theta$$

In this nomenclature the BT-cut becomes $(0, -49)^{\circ}$, and, for example, the combination $(40^{\circ}54', 16^{\circ}34')$ transforms to $(19^{\circ}06', -16^{\circ}34')$.

Table 3. Relationship Between "Rotated" and Crystal-Axes-Referred Material Constants for Quartz

$$\varepsilon'_{22} = \varepsilon_{11} \cos^2\theta + \varepsilon_{33} \sin^2\theta$$

$$e'_{22} = e_{11} \sin 3\phi \cos^3\theta$$

$$e'_{24} = -e_{11} \sin 3\phi \sin\theta \cos^2\theta$$

$$e'_{26} = -(e_{11} \cos 3\phi \cos\theta + e_{14} \sin\theta) \cos\theta$$

$$c'_{22} = c_{11} \cos^4\theta + c_{33} \sin^4\theta + (c_{13}/2 + c_{44}) \sin^2 2\theta - 2 c_{14} \cos 3\phi \sin 2\theta \cos^2\theta$$

$$c'_{24} = (1/2)[(c_{11} + c_{33}) \sin^2\theta + (c_{13} + 2 c_{44}) \cos 2\theta - c_{11}] \sin 2\theta - c_{14} \cos 3\phi \cos\theta \cos 3\theta$$

$$c'_{26} = -3 c_{14} \sin 3\phi \sin\theta \cos^2\theta$$

$$c'_{44} = c_{44} + (c_{11}/4 - c_{13}/2 + c_{33}/4 - c_{44}) \sin^2 2\theta + (1/2) c_{14} \cos 3\phi \sin 4\theta$$

$$c'_{46} = c_{14} (2 - 3 \cos^2\theta) \sin 3\phi \cos\theta$$

$$c'_{66} = c_{66} \cos^2\theta + c_{44} \sin^2\theta + c_{14} \cos 3\phi \sin 2\theta$$

4. THICKNESS VIBRATIONS OF QUARTZ

Consider thickness vibrations normal to the x_2-axis. The differential equations of motions, Eq. (6), expand to

$$\begin{aligned} \Gamma_{66}\, u_{1,22} + \Gamma_{26}\, u_{2,22} + \Gamma_{46}\, u_{3,22} &= \rho \ddot{u}_1 \\ \Gamma_{26}\, u_{1,22} + \Gamma_{22}\, u_{2,22} + \Gamma_{24}\, u_{3,22} &= \rho \ddot{u}_2 \\ \Gamma_{46}\, u_{1,22} + \Gamma_{24}\, u_{2,22} + \Gamma_{44}\, u_{3,22} &= \rho \ddot{u}_3 \end{aligned} \tag{25}$$

The appropriate "stiffened" elastic constants, referred to the crystal axes, are listed in Table 4. The three eigenvalues Γ^m are calculated by expanding the determinant derived from Eq. (11).

Table 4. "Stiffened" Elastic Constants of Quartz

$$\Gamma_{22} = [c_{11} + (e_{11}^2/\varepsilon) \sin^2 3\phi] \cos^4\theta + c_{33} \sin^4\theta + (c_{13}/2 + c_{44}) \sin^2 2\theta - 2 c_{14} \sin 2\theta \cos^2\theta \cos 3\phi$$

$$\Gamma_{44} = c_{44} \cos^2 2\theta + (1/4)[c_{11} + (e_{11}^2/\varepsilon) \sin^2 3\phi - 2 c_{13} + c_{33}] \sin^2 2\theta + (1/2) c_{14} \sin 4\theta \cos 3\phi$$

$$\Gamma_{66} = [c_{66} + (e_{11}^2/\varepsilon) \cos^2 3\phi] \cos^2\theta + (c_{44} + e_{14}^2/\varepsilon) \sin^2\theta + (c_{14} + e_{11}\, e_{14}/\varepsilon) \sin 2\theta \cos 3\phi$$

$$\Gamma_{24} = \left(\left\{-[c_{11} + (e_{11}^2/\varepsilon) \sin^2 3\phi] \cos^2\theta + (c_{13} + 2 c_{44}) \cos 2\theta + c_{33} \sin^2\theta\right\} \sin\theta - c_{14} \cos 3\phi \cos 3\theta\right) \cos\theta$$

$$\Gamma_{26} = -[(3 c_{14} + e_{11}\, e_{14}/\varepsilon) \sin\theta + (e_{11}^2/\varepsilon) \cos 3\phi \cos\theta] \sin 3\phi \cos^2\theta$$

$$\Gamma_{46} = [(3 \sin^2\theta - 1) c_{14} + (1/2)(e_{11}^2/\varepsilon) \cos 3\phi \sin 2\theta + (e_{11}\, e_{14}/\varepsilon) \sin^2\theta] \sin 3\phi \cos\theta$$

where

$$\varepsilon = \varepsilon_{11} + \varepsilon_{33} \tan^2\theta$$

$$\left|\Gamma_{pq}\right| = \begin{vmatrix} \Gamma_{66} - \Gamma & \Gamma_{26} & \Gamma_{46} \\ \Gamma_{26} & \Gamma_{22} - \Gamma & \Gamma_{24} \\ \Gamma_{46} & \Gamma_{24} & \Gamma_{44} - \Gamma \end{vmatrix} = 0 \quad , \tag{26}$$

into

$$\Gamma^3 + A_2\Gamma^2 + A_1\Gamma + A_o = 0 \tag{27}$$

where $-A_2$ is the trace, A_1 the sum of the minors of the major diagonals, and $-A_o$ the value of the determinant. The coefficients are given by

$$A_2 = -(\Gamma_{22} + \Gamma_{44} + \Gamma_{66}) \tag{28}$$

$$A_1 = (\Gamma_{22}\Gamma_{44} - \Gamma_{24}^2) + (\Gamma_{22}\Gamma_{66} - \Gamma_{26}^2) + (\Gamma_{44}\Gamma_{66} - \Gamma_{46}^2) \tag{29}$$

$$A_o = \Gamma_{22}\Gamma_{46}^2 + \Gamma_{44}\Gamma_{26}^2 + \Gamma_{66}\Gamma_{24}^2 - \Gamma_{22}\Gamma_{44}\Gamma_{66} - 2\Gamma_{24}\Gamma_{26}\Gamma_{46} \tag{30}$$

Equation (27) is solved for the three eigenvalues Γ^m by standard algebraic procedures applicable to a cubic equation with three real roots.

The three numerically ordered phase velocities are usually designated as

$$v_a > v_b > v_c$$

and are calculated from Eq. (10). Figures 2a through 2g show the angular variations of wave velocities for $\phi = 0$ to 60^o in intervals of 10^o. For these calculations we have used the c_{pq}, e_{ip}, and ε_{ij} values of BBL (1962). The types of plots shown in Figures 2a through 2g were initially published by Bechmann in 1935, republished in Ref. 6, and reprinted in Ref. 5. We include them here for reference and illustration. The numerically ordered mode designations v_a, v_b, and v_c are fairly arbitrary, as for a given ϕ the velocity curves may cross as a function of θ. This can be seen, for example, for $\phi = 60^o$, where the b- and c-modes interchange at $\theta \simeq 25^o$. The right hand side scales of Figures 2a through 2g are the frequency-thickness constants, defined as $v^m/2$, and they can be used to calculate an approximate plate thickness for a specified fundamental or overtone frequency.

---

6. Bechmann, R., Ballato, A.D., and Lukaszek, T.J. (1961) Frequency-temperature behavior of thickness modes of doubly-rotated quartz plates, 15th Annual Symposium on Frequency Control, AD 265455.

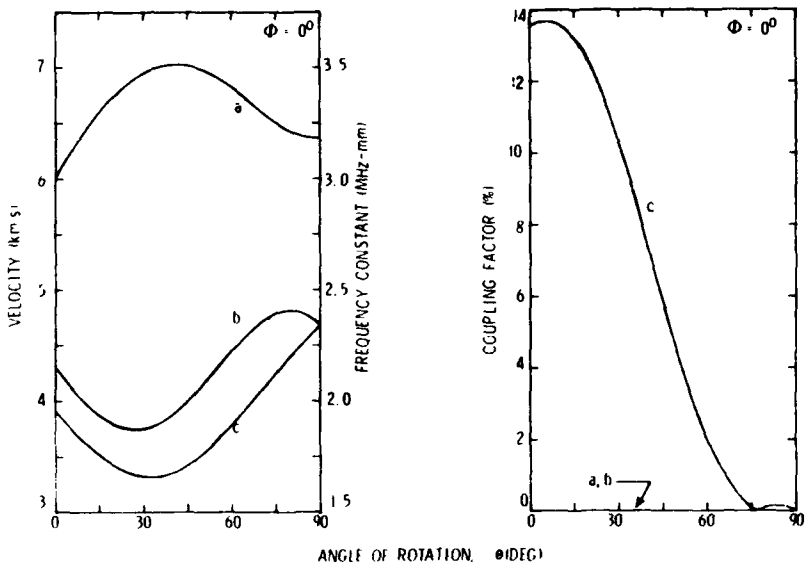

Figure 2a. Propagation Velocity, Frequency Constant, and Coupling Factor for Doubly Rotated Quartz, $\phi = 0^{o}$

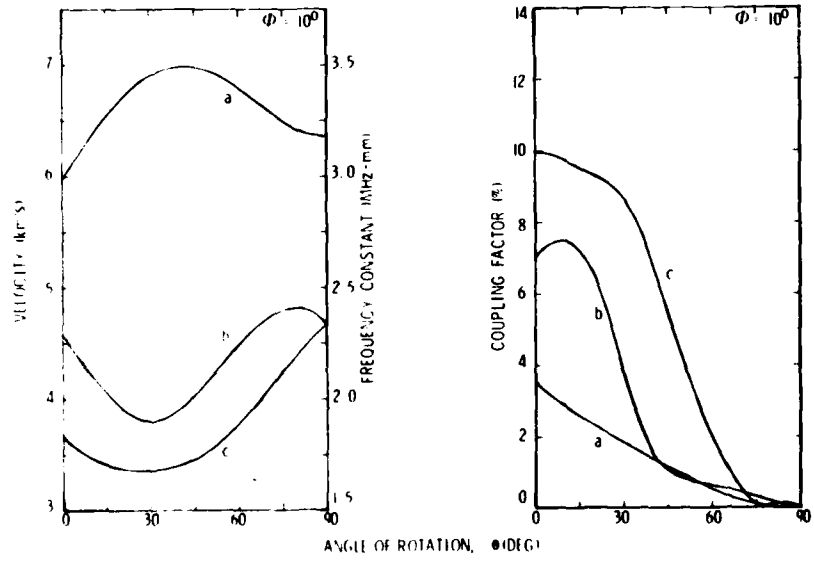

Figure 2b. Propagation Velocity, Frequency Constant, and Coupling Factor for Doubly Rotated Quartz, $\phi = 10^{o}$

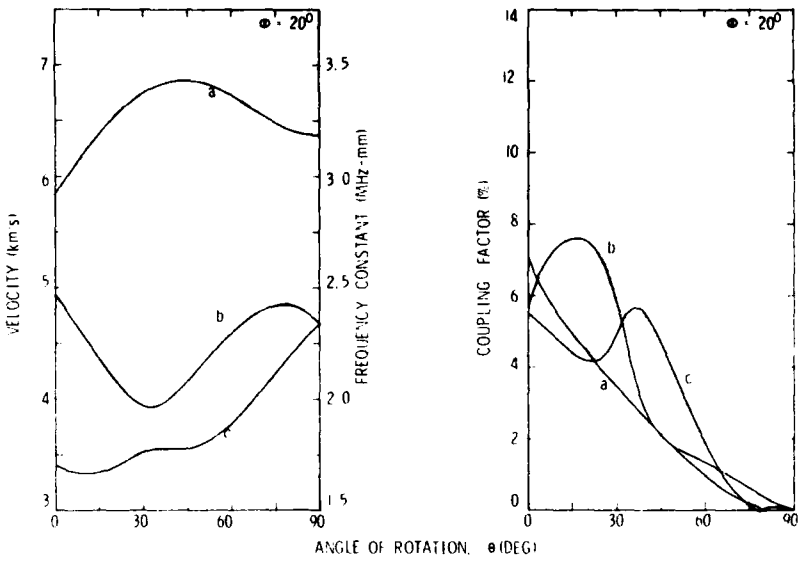

Figure 2c. Propagation Velocity, Frequency Constant, and Coupling Factor for Doubly Rotated Quartz, $\phi = 20^{\circ}$

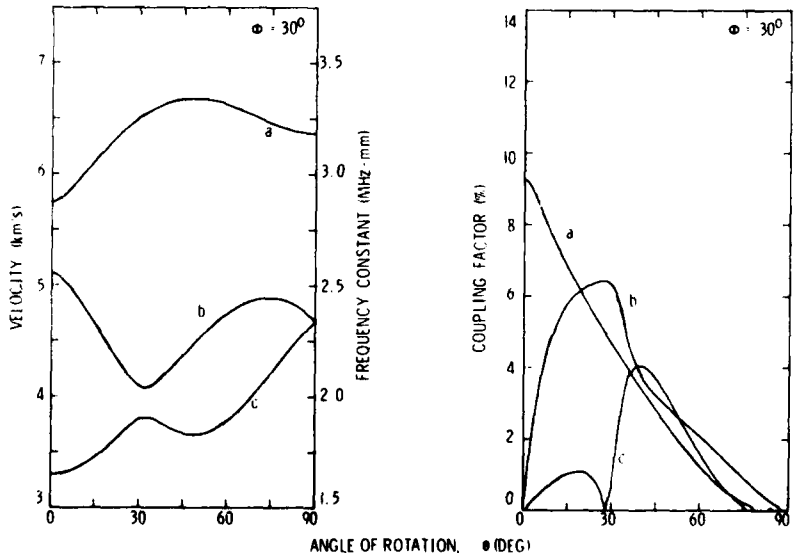

Figure 2d. Propagation Velocity, Frequency Constant, and Coupling Factor for Doubly Rotated Quartz, $\phi = 30^{\circ}$

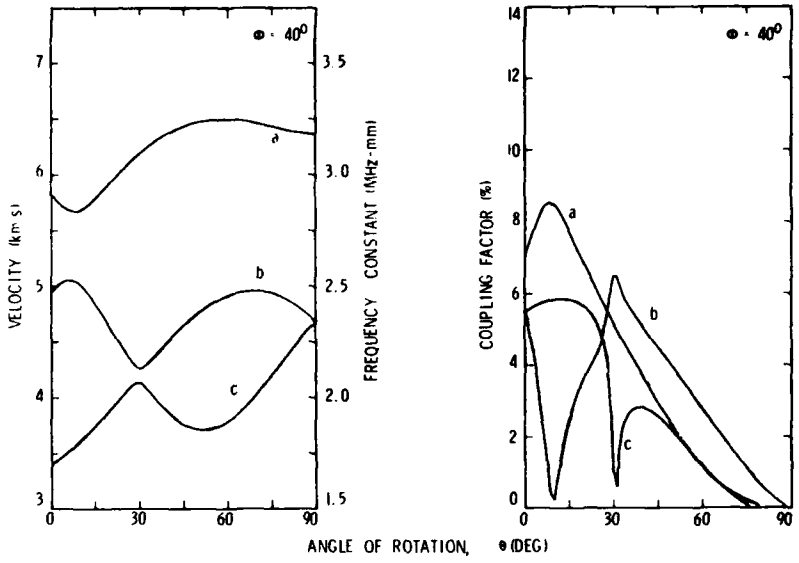

Figure 2e. Propagation Velocity, Frequency Constant, and Coupling Factor for Doubly Rotated Quartz, $\phi = 40^{\circ}$

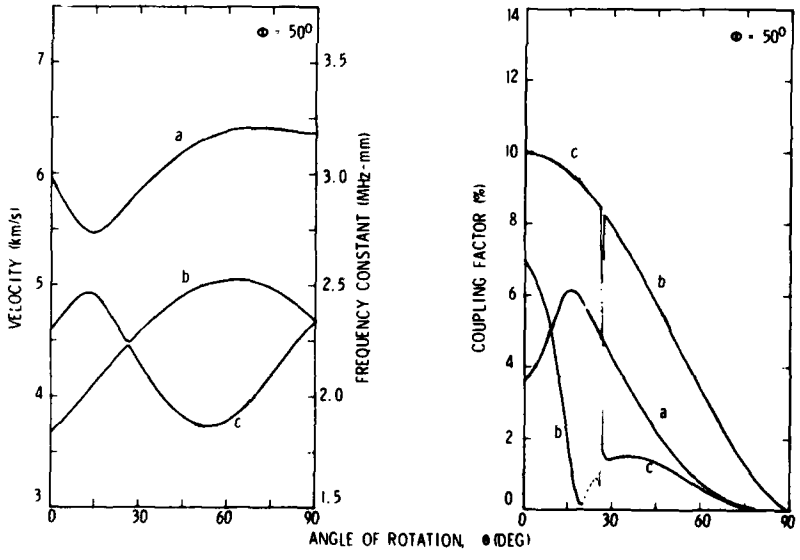

Figure 2f. Propagation Velocity, Frequency Constant, and Coupling Factor for Doubly Rotated Quartz, $\phi = 50^{\circ}$

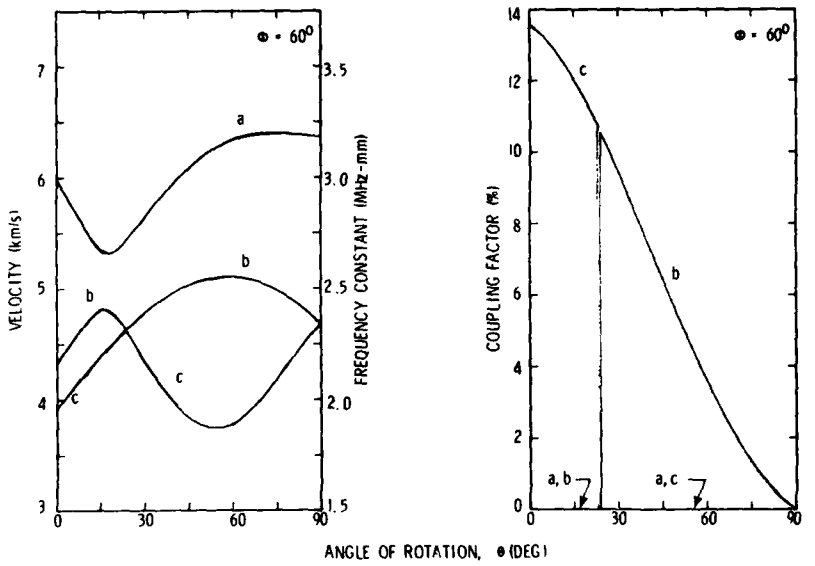

Figure 2g. Propagation Velocity, Frequency Constant, and Coupling Factor for Doubly Rotated Quartz, $\phi = 60^{\circ}$

The calculation of the electromechanical coupling factor [Eq. (15)] includes both the eigenvalues and the eigenvectors. Other eigenvalue- and eigenvector-dependent field quantities include stress, strain, electric displacement, and power density. Explicit formulas for the field quantities are given by Slobodnik, Delmonico, and Conway.[7] Standard mathematical subroutines are available at most computer installations for calculating eigenvalues and eigenvectors of any matrix type and size. For the 3 × 3 real, symmetric matrix applicable to this problem, one can derive analytic expressions for the eigenvalues and eigenvectors. This simplifies programming requirements, and computations can be performed even on hand-held or desk-top calculators.

The eigenvectors, satisfying the orthonormality

$$\beta_1^n \beta_1^m = \delta_{nm} \tag{31}$$

are derived by expanding the determinant $|\Gamma_{pq}|$ cofactors and constructing the adjoint,

---

7. Slobodnik, A.J., Delmonico, R.T., and Conway, E.D. (1980) Microwave Acoustic Handbook, Vol. 3, Bulk Wave Velocities, RADC-TR-80-188, AD A090947.

$$\Gamma_{pq} = \begin{bmatrix} (\Gamma_{22}-\Gamma)(\Gamma_{44}-\Gamma)-\Gamma_{24}^2 & \Gamma_{24}\Gamma_{26}-(\Gamma_{44}-\Gamma)\Gamma_{26} & \Gamma_{24}\Gamma_{26}-(\Gamma_{22}-\Gamma)\Gamma_{46} \\ \Gamma_{24}\Gamma_{46}-(\Gamma_{44}-\Gamma)\Gamma_{26} & (\Gamma_{44}-\Gamma)(\Gamma_{66}-\Gamma)-\Gamma_{46}^2 & \Gamma_{26}\Gamma_{46}-(\Gamma_{66}-\Gamma)\Gamma_{24} \\ \Gamma_{24}\Gamma_{26}-(\Gamma_{22}-\Gamma)\Gamma_{46} & \Gamma_{26}\Gamma_{46}-(\Gamma_{66}-\Gamma)\Gamma_{24} & (\Gamma_{22}-\Gamma)(\Gamma_{66}-\Gamma)-\Gamma_{26}^2 \end{bmatrix}$$

The three columns of the adjoint matrix give three alternate choices for the eigenvector. For our purposes we choose as the eigenvector set the linear sum of the individual columns. This choice complicates the algebraic expressions, but it avoids most of the computational difficulties encountered with degeneracies, the condition when some or all the eigenvectors vanish. The cause of the degeneracies is zero values for the off-diagonal elements Γ_{24}, Γ_{26}, or Γ_{46}. For a particular eigenvalue $\Gamma^{(m)}$, we construct the eigenvector

$$\begin{bmatrix} \phi_1^{(m)} \\ \phi_2^{(m)} \\ \phi_3^{(m)} \end{bmatrix} = (s^{(m)})^{-1/2} \begin{bmatrix} A_3^{(m)} \\ A_4^{(m)} \\ A_5^{(m)} \end{bmatrix} \tag{32}$$

where

$$\begin{aligned} A_3^{(m)} &= (\Gamma_{22}-\Gamma_{26}-\Gamma^{(m)})(\Gamma_{44}-\Gamma_{46}-\Gamma^{(m)}) - (\Gamma_{24}-\Gamma_{26})(\Gamma_{24}-\Gamma_{46}) \\ A_4^{(m)} &= (\Gamma_{44}-\Gamma_{24}-\Gamma^{(m)})(\Gamma_{66}-\Gamma_{26}-\Gamma^{(m)}) - (\Gamma_{46}-\Gamma_{24})(\Gamma_{46}-\Gamma_{26}) \\ A_5^{(m)} &= (\Gamma_{66}-\Gamma_{46}-\Gamma^{(m)})(\Gamma_{22}-\Gamma_{24}-\Gamma^{(m)}) - (\Gamma_{26}-\Gamma_{46})(\Gamma_{26}-\Gamma_{24}) \end{aligned} \tag{33}$$

and the normalization length $s^{(m)}$ is

$$s^{(m)} = (A_3^{(m)})^2 + (A_4^{(m)})^2 + (A_5^{(m)})^2 \tag{34}$$

The electromechanical coupling factor becomes

$$k^{(m)} = (e'_{26} A_3^{(m)} + e'_{22} A_4^{(m)} + e'_{24} A_5^{(m)}) (\varepsilon'_{22} \Gamma^{(m)} s^{(m)})^{-1/2} \tag{35}$$

The $k^{(m)}$ values are plotted, for illustration and reference, in the right hand side of Figures 2a through 2g.

The equations derived in this section are analytic and self-consistent. Given the material constants, one calculates for the particular angular orientation (ϕ, θ) of interest, the "stiffened" elastic constants from Table 4, solves the cubic equation, Eq. (27), for the eigenvalues Γ^m, and finds the coupling factors k^m from Eqs. (33)-(35). This then provides a convenient formalism to calculate the thickness vibration propagation velocities and electromechanical coupling factors for any doubly rotated quartz plate.

In this section we have derived the velocities by considering the wave propagation along the x_2-axis. An alternate formulation, carried out by Slobodnik et al,[7] considers the transverse propagation along the x_1-axis. The results are identical, but the pq subscripts differ. The relationship between the two formulations is given in Appendix A.

5. UNCOUPLED MODES OF VIBRATION

The eigenvalue determinant [Eq. (26)] can also be expanded into

$$(\Gamma_{22} - \Gamma)(\Gamma_{44} - \Gamma)(\Gamma_{66} - \Gamma) - \Gamma_{46}^2(\Gamma_{22} - \Gamma) - \Gamma_{26}^2(\Gamma_{44} - \Gamma) - \Gamma_{24}^2(\Gamma_{66} - \Gamma) - 2\,\Gamma_{24}\Gamma_{26}\Gamma_{46} = 0 \tag{36}$$

When any two of the three off-diagonal elements vanish, the equation factors into a linear and quadratic term in Γ. The factored equations are listed in Table 5.

If two of the off-diagonal elements vanish, the three vibration eigenvalues corresponding to m = 1, 2, and 3, are given by

$$\Gamma^{(1)};\ \Gamma^{(2)} = (1/2)(\Gamma_{pp} + \Gamma_{qq}) \pm (1/2)[(\Gamma_{pp} - \Gamma_{qq})^2 + 4\Gamma_{pq}^2]^{1/2} \tag{37}$$

and

$$\Gamma^{(3)} = \Gamma_{rr} \tag{38}$$

where p, q, and r are permutations of 2, 4, and 6. The (ϕ, θ) combinations that satisfy $\Gamma_{pq} = 0$ can be evaluated from the expressions given in Table 4. Figure 3 is a plot of these solutions using the material constants given in BBL (1962). In Figure 3, the overlapping curves at $\phi = 0$ and 60° and at $\theta = 90^\circ$ are displaced for clarity.

Table 5. Factors of Wave Velocity Eigenvalue Equation

$\Gamma_{pq} = 0$	$f(\Gamma) = 0$
$\Gamma_{24} = \Gamma_{26} = 0$	$(\Gamma_{22} - \Gamma)\left[(\Gamma_{44} - \Gamma)(\Gamma_{66} - \Gamma) - \Gamma_{46}^2\right] = 0$
$\Gamma_{24} = \Gamma_{46} = 0$	$(\Gamma_{44} - \Gamma)\left[(\Gamma_{22} - \Gamma)(\Gamma_{66} - \Gamma) - \Gamma_{26}^2\right] = 0$
$\Gamma_{26} = \Gamma_{46} = 0$	$(\Gamma_{66} - \Gamma)\left[(\Gamma_{22} - \Gamma)(\Gamma_{44} - \Gamma) - \Gamma_{24}^2\right] = 0$
$\Gamma_{24} = \Gamma_{26} = \Gamma_{46} = 0$	$(\Gamma_{22} - \Gamma)(\Gamma_{44} - \Gamma)(\Gamma_{66} - \Gamma) = 0$

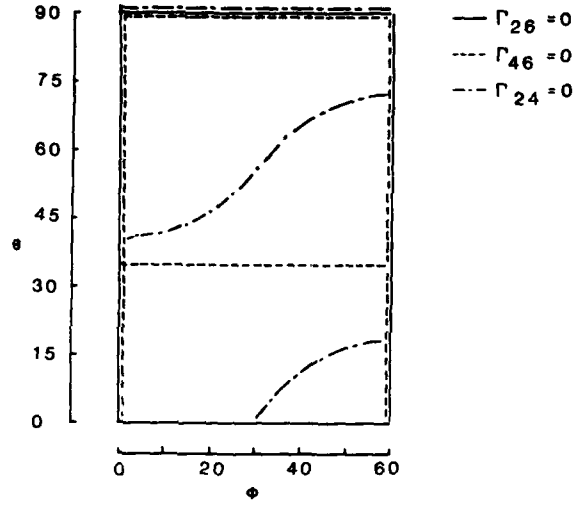

Figure 3. Zero Values of Off-Diagonal Matrix Elements, $\Gamma_{pq} = 0$

We note that $\Gamma_{24} = 0$ is satisfied by $(\phi, 90)^\circ$, that is, for any ϕ at $\theta = 90^\circ$. It is also satisfied by a continuous function between $\phi = 0$ and 60°, with end points $(0, 40.8)^\circ$ and $(60, 72.4)^\circ$, and by a third branch continuous between $(30, 0)^\circ$ and $(60, 17.7)^\circ$.

$\Gamma_{26} = 0$ is satisfied by any θ at $\phi = 0$ and 60°, and for any ϕ at $\theta = 90^\circ$, that is, $(0, \theta)^\circ$, $(60, \theta)^\circ$, and $(\phi, 90)^\circ$. In addition, the bracketed term of Γ_{26}, listed in Table 4, yields a slowly varying function, symmetric around $(30, 0)^\circ$ and increasing to $\theta = 0.8^\circ$ at $\phi = 0$ and 60°. The deviation from $(\phi, 0)^\circ$ is due to the small contribution of the piezoelectric constants to the bracketed term.

$\Gamma_{46} = 0$ has solutions $(0, \theta)^\circ$, $(60, \theta)^\circ$, and $(\phi, 90)^\circ$. The bracketed term yields a continuous function between $(0, 35.5)^\circ$ and $(60, 34.9)^\circ$. The small variations in θ are again due to piezoelectric effects. If we neglect piezoelectric effects we obtain $(\phi, 35.26)^\circ$, which is exactly the AT-cut angle. It is uncertain whether this is a pure coincidence, or is a contributing factor in determining the position of the AT-cut.

The overlap, or intersection, of two or three solutions of $\Gamma_{pq} = 0$ gives the uncoupled modes of vibration. From the diagram depicted in Figure 3, these directions are given by $(0, \theta)^\circ$, $(60, \theta)^\circ$, $(\phi, 90)^\circ$, and $(30, 0)^\circ$. One of the problems associated with the preferred directions is that the piezoelectrically "stiffened" elastic constant, defined by Eq. (5), may no longer be "stiffened", has no piezoelectric coupling, and cannot be excited by piezoelectric means. An inspection of Table 4 shows that for Γ_{22}, Γ_{44}, and Γ_{24}, the term containing the piezoelectric constant is multipled by a $\sin^2 3\phi$ factor, which vanishes both at $\phi = 0$ and 60°. Thus at $(0, \theta)^\circ$ and $(60, \theta)^\circ$ two of the modes are piezoelectrically inactive, and at $(\phi, 90)^\circ$ none of the modes can be excited by an alternating voltage applied to the electrodes.

McSkimin[3] has evaluated the elastic constants from ultrasonic excitation. He selected $(0, 0)^\circ$, $(0, 90)^\circ$, and $(30, 0)^\circ$. At these points, the three modes of vibrations reduce to values listed in Table 6. The choice of $(0, 90)^\circ$ is not unique. Any $(\phi, 90)^\circ$ will give a doubly degenerate $\Gamma^{(1)} = \Gamma^{(2)} = c_{44}$ and $\Gamma^{(3)} = c_{33}$. Similarly, $(0, 0)^\circ$ and $(60, 0)^\circ$ yield identical values. From the angular orientation chosen by McSkimin one can evaluate $e_{11}^2/\varepsilon_{11}$ and all elastic constants except c_{13}. The determination of c_{13} involves four other elastic constants, and, depending on accumulation or cancellation of experimental errors, may be the least accurate. By the same token, c_{33} and c_{44} should be very accurate. For c_{13} McSkimin chose $(0, 45)^\circ$, at which point

$$c_{13} = (c_{14} - c_{44}) + \{[2\Gamma - (c_{33} + c_{44})][2\Gamma - (c_{11} - 2c_{14} + c_{44})]\}^{1/2} \qquad (39)$$

but any other angular orientation will result in similar complexity.

If one is restricted to determining the material parameters from piezoelectric excitation, for example, from frequencies derived from resonators or disks in dielectric gap holders, the key equation determining the angular cuts is

$$\Gamma^{(3)}(0,\theta);\ \Gamma^{(3)}(60,\theta) = (c_{66} + e_{11}^2/\varepsilon)\cos^2\theta + (c_{44} + e_{14}^2/\varepsilon)\sin^2\theta$$
$$\pm (c_{14} + e_{11}e_{14}/\varepsilon)\sin 2\theta \qquad (40)$$

where the plus sign applies to $\phi = 0$, and the minus sign to $\phi = 60^{\circ}$. The proper selection of θ at $\phi = 0$ and 60° will yield c_{14}, c_{44}, c_{66}, the piezoelectric, and the dielectric constants. It is especially important to have identical θ-angle cuts for both $\phi = 0$ and 60°. This allows simplifications in terms of $\Gamma^{(3)}(0, \theta) \pm \Gamma^{(3)}(60, \theta)$. As before, c_{11} is determined from $(30, 0)^{\circ}$, but neither c_{13} nor c_{33} are accessible to uncoupled mode piezoelectric excitation.

Table 6. Eigenvalues Γ^{m} for Highly Symmetric (ϕ, θ) Orientations

(ϕ, θ)	$\Gamma^{(1)}; \Gamma^{(2)}$	$\Gamma^{(3)}$
(0, 0) and (60, 0)	$(1/2)\{(c_{11}+c_{44}) \pm [(c_{11}-c_{44})^2+4c_{14}^2]^{1/2}\}$	$c_{66} + e_{11}^2/\varepsilon_{11}$
$(\phi, 90)$	c_{44}	c_{33}
(30, 0)	$(1/2)\{(c_{44}+c_{66}) \pm [(c_{44}-c_{66})^2+4c_{14}^2]^{1/2}\}$	$c_{11} + e_{11}^2/\varepsilon_{11}$

6. EXPERIMENTAL VALUES OF ELASTIC CONSTANTS OF QUARTZ

Currently, the most widely accepted c_{pq} values are the ones derived by McSkimin[3] and independently by BBL (1962), and these are in general agreement with previous investigations. In Table 7, under the heading "Observed", we list the experimental data sets of both investigations, and in Table 8, we list the derived elastic coefficients. The differences between the McSkimin and BBL derived values are small, and either set can be used equally well to calculate appropriate quantities of interest. In Table 8, we also include the other material properties needed for calculating the transverse wave propagation of quartz. Unless otherwise specified, these are taken from BBL (1962).

In Table 7, under the heading "BBL (1962)", we list three sets of calculated values. The first column is taken from BBL (1962), and the second column, "This Work I", is calculated in this investigation, using BBL (1962) derived constants. The slight differences in values are due to the fact that BBL (1962) calculations are based on a "semi-stiffened" elastic constant,

$$\Gamma_{pq} = (c_{pq} + e_{2p}\, e_{2q}/\varepsilon_{22})'$$

rather than the rigorous definition, Eq. (5),

$$\Gamma_{pq} = c'_{pq} + e'_{2p} e'_{2q} / \epsilon'_{22} \quad .$$

Table 7. Measured and Calculated Velocities for Doubly Rotated Quartz Orientations

Orientation Angles ϕ	θ	Mode (cut)	Velocity Data (m/sec) BBL (1962) Obs.	BBL (1962) Calculated BBL	This Work I	This Work II	McSkimin[3] Obs.	McSkimin[3] Calc.
0	0	a(Y)					6006	6005
0	0	b(Y)					4323	4322
0	0	c(Y)	3892	3914	3915	3901	3918	3917
0	$35^{\circ}15'$	c(AT)	3320	3320	3322	3246		
0	45	a					7121	7021
0	45	b					3981	3981
0	45	c					3427	3427
0	90	a(Z)					6319	6319
0	90	b, c(Z)					4687	4688
20	$34^{\circ}20'$	c(IT)	3386	3566	3551	3467		
30	0	a(X)	5690	5746	5746	5643	5749	5749
30	0	b(X)					5114	5114
30	0	c(X)					3298	3298
30	10	a	5780	5960	5956	5830		
30	30	b	4096	4100	4097	4104		
45	34.5°	c(RT)	4080	4094	4080	4117		
45	35	b	4416	4540	4533	4417		
47.5°	33	c	4202	4176	4162	4205		
50	32	c	4212	4240	4223	4271		
50	33	c	4316	4200	4183	4228		
50	38	b	4694	4776	4767	4684		
55	47	b	5038	5030	5021	5004		
60	$49^{\circ}13'$	b(BT)	5080	5060	5072	5089		
Number of test points				14			11	
Least Square Variance				7570	7186	2198		0.5

Table 8. Elastic Constants of Quartz

pq	c_{pq} in units of 10^9 N/m^2			
		BBL (1962) Data		
	McSkimin	BBL	This Work	BBL (1961)
11	86.80	86.74	83.63	86.3
13	11.91	11.91	-0.88	6.3
14	-18.04	-17.91	-18.88	-17.1
33	105.75	107.2	77.60	90.3
44	58.20	57.94	57.32	66.0
66	39.88	39.88	39.58	32.2

$e_{11} = 0.171\ e_{14} = -0.0406$ (C/m^2)

$\varepsilon_{11} = 39.21 \times 10^{-12}$ $\varepsilon_{33} = 41.03 \times 10^{-12}$ (F/m)

$e_{11}^2/\varepsilon_{11} = 0.77 \times 10^9$ (N/m^2) (McSkimin)

$\rho = 2650$ kg/m^3 (BBL); 2648.5 kg/m^3 (McSkimin)

McSkimin et al[8] have applied a least squares minimization to the experimental data, and the derived c_{pq} values in Table 8 are the result of this analysis. They minimized the variance

$$\sigma^2 = (1/n) \sum_{i=1}^{n} G_i (v_{exp} - v_{calc})_i^2 \qquad (41)$$

where the summation is over the number of experimental points n. The weighting factor G_i is either $G_i = 1$ or $G_i = 1/v_{exp}^2$. If the experimental points are equally reliable on an absolute basis, then $G_i = 1$ is the appropriate choice. If the experimental points are equally valid on a percentage basis, one chooses $G_i = 1/v_{exp}^2$. For this data set, the differences between the two approaches are insignificant.

8. McSkimin, H.J., Andreatch, P., and Thurston, R.N. (1965) Elastic moduli of quartz versus hydrostatic pressure at 25°C and -195.8°C, J. Appl. Phys. 36:1624-1632.

The variances for the various data sets are listed at the bottom of Table 7. The listed velocity values are rounded off to the nearest integer, whereas the computations were carried out to the appropriate number of decimal places. Hence there are small differences between the listed variances and ones computed from the listed velocities. The close agreement between calculated and experimental velocities for the McSkimin data, as reflected in $\sigma^2 = 0.5$, is not surprising. McSkimin used 10 of the 11 test points to derive 6 c_{pq} values and $e_{11}^2/\varepsilon_{11}$, and one does expect a close fit. It is more questionable whether 7 fitting parameters and 10 data points constitute a statistically significant set, especially if these points are chosen along the uncoupled directions.

The variance of the BBL data set, using BBL (1962) derived material constants, is $\sigma^2 = 7186$. BBL (1962) have not performed a least squares analysis to their 14 point data set, and from their publication the methodology used to derive c_{pq} is unclear. We have subjected the BBL data set to a least squares minimization routine, and the results of the best fit to the experimental data are listed in Table 7 under "This Work II" and in Table 8 under "This Work". We note that the least squares fit analysis reduces the initial $\sigma^2 = 7186$ to $\sigma^2 = 2198$, with corresponding differences in c_{pq}. The major c_{pq} changes occur in c_{13} and c_{33}, the two constants not accessible to uncoupled mode piezoelectric excitation.

We have performed several computational efforts trying to improve the BBL (1962) data fit. One included the assumption that one of the 14 test points is inaccurate. We systematically neglected one test point at a time, and re-fitted the data. There were some improvements, but none of them dramatic. The best initial 13 point data fit is obtained by omitting $(30, 10)^\circ$, with the variance reduced to $\sigma^2 = 5363$, and the best final fit is obtained by neglecting the AT-cut $(0, 35.25)^\circ$, with $\sigma^2 = 1360$. However, the AT-cut is the point that BBL (1962) assumes to be in perfect coincidence. Another supposition was that BBL (1962) has mislabeled one of the modes. The mode assignment of each test point was systematically changed, one at a time, and the data re-fitted. In all cases the initial $\sigma^2 = 7186$ value increased, confirming the accuracy of the BBL (1962) mode assignments.

There is another BBL data set, Ref. 6, designated as BBL (1961), consisting of 17 rotations with 47 test points. Some test points of the two sets are identical, and some are listed in BBL (1962) with slightly different θ-angles. Also, all (ϕ, θ) combinations of this data set are given as integers, without any error bars, a highly unrealistic situation. Nevertheless, we have performed a least square minimization of the 47 test points and the initial $\sigma^2 = 5840$ can be reduced to $\sigma^2 = 2903$, the same order of magnitude as the BBL (1962) data fit. The corresponding c_{pq} values for this fit are listed in Table 8 under "BBL (1961)".

7. ANALYSIS AND CONCLUSIONS

The knowledge of the elastic constants of quartz and their temperature coefficients is imperative in describing the frequency and temperature response of the resonator device. In addition to the elastic constants c_{pq}, BBL (1962) also derived first, second, and third order temperature coefficients of the elastic constants, $T_n(c_{pq})$, n = 1, 2, and 3, from a set of 23-24 crystallographically doubly rotated resonators. The coefficients were obtained by fitting the static frequency-temperature curves in the -200 to +200°C range by the cubic $T_n(f)(T - T_o)^n$ relationship, where $T_n(f)$ are the temperature coefficients of frequency. We have shown that there are serious discrepancies in the original analysis of the BBL (1962) data set, and this raises issues regarding the applicability of currently accepted c_{pq} and $T_n(c_{pq})$ values to crystallographically doubly rotated cuts.

The large differences in c_{33} are especially disturbing. This constant, as indicated in Table 6, is the easiest to determine by non-piezoelectric means from $(\phi, 90)^o$, and it should be the most accurate. Yet, it shows the largest variation when computed from an arbitrary, crystallographically doubly rotated, piezoelectrically excited resonator set. At the same time, c_{44}, computed by the same technique from $(\phi, 90)^o$, does agree very well.

Our major concern regarding $T_n(c_{pq})$ relates to the fact that the computation of the first, second, and third order temperature coefficient involves a knowledge of the elastic constants, and that the higher order coefficients also depend on the values of the lower order coefficients. Errors are cumulative, and c_{pq} inaccuracies are reflected in all temperature coefficients. Similarly, $T_1(c_{pq})$ errors invalidate $T_2(c_{pq})$ results, and these in turn affect $T_3(c_{pq})$. The BBL (1962) derived temperature coefficients are often in sharp disagreement with previous results, but are claimed to be more accurate than ones determined by earlier investigators. The problems associated with the BBL (1962) data set regarding agreement with accepted c_{pq} values raises more serious questions with respect to the BBL (1962) derived temperature coefficients.

There are several possibilities which may account for the BBL (1962) discrepancies. Strictly speaking, the derived material constants are not necessarily the intrinsic values and their applicability to other situations needs to be established. Geometric factors may influence results, and sets of values derived from one configuration and experimental procedure may not automatically be applied to other modes of operation. Adams et al[9] also derived a set of temperature

9. Adams, C.A., Enslow, G.M., Kusters, J.A., and Ward, R.W. (1970) Selected topics in quartz crystal research, 24th Annual Symposium on Frequency Control, AD 746210.

coefficients of elastic constants, and they caution that their $T_n(c_{pq})$ data is "exactly applicable to crystals having the same physical characteristics as the ones in this study; that is, same diameter, thickness, contour, etc." BBL (1963), Ref. 10 also lists factors that influence the temperature-frequency behavior of the resonator.

McSkimin's experiments were carried out on 0.5-cubic-inch quartz samples, whereas BBL obtained the material from several sources. The BBL crystals had large thickness to diameter ratio variations, and included plano-plano, beveled at the edges, and plano-convex geometries. Sample set divergencies extended to fabrication processes, support structure, electrode size, air gap holder and resonator enclosure, drive level, and operations at different overtones, all of which affect the measured frequencies. Recent discussions with A. Ballato tend to support the argument that for the BBL sample set they lacked an accurate knowledge of (ϕ, θ). The oriented plates and finished resonators were acquired from outside sources, and there was no independent check on (ϕ, θ).

Another possibility for the discrepancies relates to the fact that we are trying to apply the theoretical formulation of an infinite plate to a finite electroded disk. This is very simplistic approach that works well when symmetries cancel a large number of terms, but does not describe the realities of doubly rotated disks. It is then not too surprising that this mixture of geometrical configurations, experimental procedures, and simplistic mathematical model yields large variances, and deviations from predicted results can always be attributed to some of these factors.

We are confronted with two issues: (1) the validity of the BBL (1962) determined c_{pq} owing to the large variance associated with the data set, and (2) that the number of points, 14, used to derive the least square fit c_{pq} set in this investigation, is still statistically insignificant. Consequently, despite the reduced variance, there is no assurance that this c_{pq} set gives a more realistic prediction of the frequencies of doubly rotated cuts. The BBL (1962) c_{pq} values, confirmed by independent measurements by McSkimin, are in general agreement with previous data accumulated by many investigators over the last 50-70 years. However, all previous investigations utilized uncoupled mode orientations, and, to the best of our knowledge, BBL (1962) was the first group trying to derive c_{pq} from widely rotated (ϕ, θ) cuts. Thus, despite all the reservations, one is forced, at the present time, to retain and accept the BBL (1962), or the McSkimin, c_{pq} values. In this context, the least squares fit derived c_{pq}, listed in Table 8, can

---

10. Bechmann, R., Ballato, A.D., and Lukaszek, T.J. (1963) Higher-Order Temperature Coefficients of the Elastic Stiffnesses and Compliances of α-Quartz, USAELRDL TR 2261.

be regarded as an indication that, despite all previous work on this subject, the derived c_{pq} are inconsistent.

This investigation points out the need for the experimental redetermination of the elastic constants of quartz and their temperature coefficients on geometrically consistent sample sets, on a statistically significant number of doubly rotated crystals, bulk and disk configurations, air gap and resonator enclosures, and piezoelectric and other means of excitations. It also calls for detailed documentation of sample and experimental procedures. A new experimental investigation will also afford the opportunity to evaluate novel factors, discovered during the last twenty years, which influence resonator behavior.

References

1. Tiersten, H.F. (1969) Linear Piezoelectric Plate Vibrations, Plenum Press, pp. 88-93.
2. Cady, W.G. (1964) Piezoelectricity, Dover Publications, Vol. I, pp. 134-157.
3. McSkimin, H.J. (1962) Measurement of the 25°C zero-field electric moduli of quartz by high frequency plane-wave propagation, J. Acoust. Soc. Am. 34:1271-1274.
4. Bechmann, R., Ballato, A.D., and Lukaszek, T.J. (1962) Higher-order temperature coefficients of the elastic stiffnesses and compliances of alpha-quartz, Proc. of the IRE 50:1812-1822.
5. Ballato, A. (1977) Doubly rotated thickness mode plate vibrators, Physical Acoustics, XIII, W. P. Mason and R. N. Thurston, Eds., Academic Press, New York, pp. 115-181.
6. Bechmann, R., Ballato, A.D., and Lukaszek, T.J. (1961) Frequency-temperature behavior of thickness modes of doubly-rotated quartz plates, 15th Annual Symposium on Frequency Control, AD 265455.
7. Slobodnik, A.J., Delmonico, R.T., and Conway, E.D. (1980) Microwave Acoustic Handbook, Vol. 3, Bulk Wave Velocities, RADC-TR-80-188, AD A090947.
8. McSkimin, H.J., Andreatch, P., and Thurston, R.N. (1965) Elastic moduli of quartz versus hydrostatic pressure at 25°C and -195.8°C, J. Appl. Phys. 36:1624-1632.
9. Adams, C.A., Enslow, G.M., Kusters, J.A., and Ward, R.W. (1970) Selected topics in quartz crystal research, 24th Annual Symposium on Frequency Control, AD 746210.
10. Bechmann, R., Ballato, A.D., and Lukaszek, T.J. (1963) Higher-Order Temperature Coefficients of the Elastic Stiffnesses and Compliances of α-Quartz, USAELRDL TR 2261.

Appendix A

Transverse Vibrations Along the x_1-Axis

Slobodnik, Delmonico, and Conway[7] define the acoustic wave propagation in terms of a fixed coordinate system (x, y, z) rotated axes (1, 2, 3), Euler rotation angles (λ, μ, θ), and a phase velocity vector that always propagates along the 1-axis. We wish to specialize the Euler angles to describe a doubly rotated Y-plate with its thickness direction normal to the y-axis, and with rotation angles (ϕ, θ), as depicted in Figure 1.

The first Euler angle λ denotes a rotation around the z-axis, the second Euler angle μ denotes a rotation around the 1-axis, that is, the rotated x-axis, and the third Euler angle θ denotes a rotation around the 3-axis, that is, the rotated z-axis. In this formulation, the initial position of the plate, depicted in Figure A1.a, is that of an X-plate, thickness direction normal to the crystallographic x-axis. The angle $\lambda = 90^{\circ}$ rotates the X-plate into a Y-plate. For our purposes, $\lambda = 90 + \phi$. This rotates the X-plate past the Y-plate position, and ϕ becomes the rotation angle of the Y-plate around the z-axis. The position of the coordinate system after the first Euler angle rotation is depicted in Figure A1.b. The second Euler angle μ is a rotation around the 1-axis. This angle has to be chosen in a manner that will align the 3-axis with the x-y plane. This is necessary since the third Euler angle θ, rotation around the 3-axis, must be identical with the x'-axis rotation depicted in Figure 1, and the x'-axis lies in the x-y plane. μ is then chosen as $\mu = 90^{\circ}$, and the position of the coordinate system after the second Euler angle rotation is depicted in Figure A1.c. The position of the coordinate

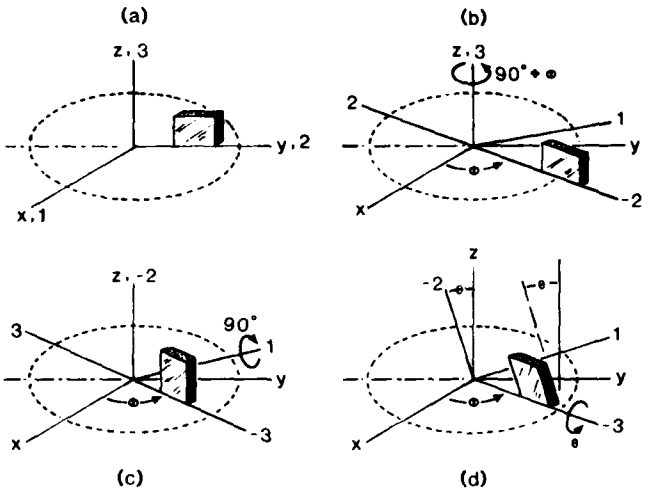

Figure A1. Euler Angles for Rotated Y-cut Plate

system after the third Euler angle rotation, a rotation θ around the 3-axis, is depicted in Figure A1.d.

The Euler angles for a doubly rotated Y-plate are then given by

$$(\lambda, \mu, \theta) = (90 + \phi, 90, \theta) \tag{A1}$$

For these angles the Euler transformation matrix reduces to

$$V_{ij} = \begin{bmatrix} -\sin\phi\cos\theta & \cos\phi\cos\theta & \sin\theta \\ \sin\phi\sin\theta & -\cos\phi\sin\theta & \cos\theta \\ \cos\phi & \sin\theta & 0 \end{bmatrix} \tag{A2}$$

The rotated material properties ε'_{ij}, e'_{ip}, and c'_{pq} are then determined from Eqs. (19)-(21) and transformation matrix of Eq. (A2). Slobodnik has not derived explicit algebraic expressions for the rotated properties, but numerical results can be easily generated by computerized DO LOOP techniques. It can be shown that there is equivalence between the expressions listed in Table 3 and the ones derived from Eq. (A2). Table A1 lists the notations of this equivalence.

Table A1. Comparison of "Rotated" Material Constants

This Work	Slobodnik
c'_{22}	c'_{11}
c'_{24}	c'_{16}
c'_{26}	c'_{15}
c'_{44}	c'_{66}
c'_{46}	c'_{56}
c'_{66}	c'_{55}
e'_{22}	e'_{11}
e'_{24}	e'_{16}
e'_{26}	e'_{15}
ε'_{22}	ε'_{11}

For propagation along the x_1-axis, the eigenvalue determinant, Eq. (11), is expanded with $\nu = 1$, and one obtains

$$\begin{bmatrix} \Gamma_{11} - \Gamma & \Gamma_{16} & \Gamma_{15} \\ \Gamma_{16} & \Gamma_{66} - \Gamma & \Gamma_{56} \\ \Gamma_{15} & \Gamma_{56} & \Gamma_{55} - \Gamma \end{bmatrix} = 0 \tag{A3}$$

The coefficients of the eigenvalue equation

$$\Gamma^3 + A_2\Gamma^2 + A_1\Gamma + A_0 = 0 \tag{A4}$$

become

$$A_2 = -(\Gamma_{11} + \Gamma_{55} + \Gamma_{66}) \tag{A5}$$

$$A_1 \quad (\Gamma_{11}\Gamma_{55} - \Gamma_{15}^2) + (\Gamma_{11}\Gamma_{66} - \Gamma_{16}^2) + (\Gamma_{55}\Gamma_{66} - \Gamma_{56}^2) \tag{A6}$$

$$A_o = \Gamma_{11}\Gamma_{56}^2 + \Gamma_{55}\Gamma_{16}^2 + \Gamma_{66}\Gamma_{15}^2 - \Gamma_{11}\Gamma_{55}\Gamma_{66} - 2\Gamma_{15}\Gamma_{16}\Gamma_{56} \tag{A7}$$

The comparative notations listed in Table A1 show that, in terms of rotation angles and material properties referred to the crystallographic axes, both formulations give identical numerical coefficients for the cubic equation, and the eigenvalues will be the same.

MISSION
of
Rome Air Development Center

RADC plans and executes research, development, test and selected acquisition programs in support of Command, Control, Communications and Intelligence (C3I) activities. Technical and engineering support within areas of competence is provided to ESD Program Offices (POs) and other ESD elements. The principal technical mission areas are communications, electromagnetic guidance and control, surveillance of ground and aerospace objects, intelligence data collection and handling, information system technology, ionospheric propagation, solid state sciences, microwave physics and electronic reliability, maintainability and compatibility.

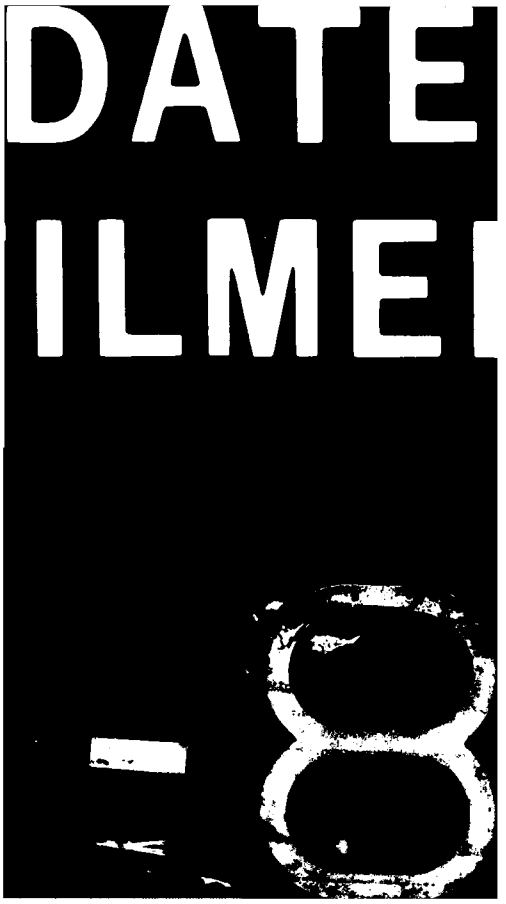
DATE
ILME